

# Dynamics and structure in a model of two-dimensional supercooled liquid molecules

Andrew Ton

February 7, 2019

## Contents

<b>1</b>	<b>Introduction: What are supercooled liquids?</b>	<b>2</b>
1.1	Ordinary liquids, crystals, and glasses . . . . .	2
1.1.1	Mechanical differences . . . . .	2
1.1.2	Structural similarities . . . . .	2
1.1.3	Thermodynamic signatures . . . . .	2
<b>2</b>	<b>Model details</b>	<b>3</b>
2.1	Finite size . . . . .	4
<b>3</b>	<b>Structure</b>	<b>4</b>
3.1	Looking at the configurations . . . . .	4
3.2	Hexatic order . . . . .	4
3.3	Pair correlation functions . . . . .	6
3.3.1	Hexatic pair correlation function . . . . .	7
3.3.2	Static structure factor . . . . .	9
<b>4</b>	<b>Dynamics</b>	<b>11</b>
4.1	Mean square displacement . . . . .	11
4.1.1	Calculating the diffusion coefficient . . . . .	11
4.2	Body-orientational time correlation functions . . . . .	12
4.2.1	Single and collective hexatic body-orientational time correlation function . . . . .	13
4.3	Incoherent intermediate scattering function . . . . .	13

# 1 Introduction: What are supercooled liquids?

Supercooled liquids are liquids **below** their freezing temperature. Alternatively, the supercooled regime of a liquid can be operationally defined as the region in a phase diagram where a liquid's relaxation times begin to diverge. Supercooled liquids are metastable with respect to a crystalline phase, always on the verge of falling out of thermodynamic equilibrium. <sup>1</sup>

## 1.1 Ordinary liquids, crystals, and glasses

Preparing a supercooled liquid is a delicate process, and one worries that improper handling of a supercooled liquid may instead lead to other materials. The unwanted products can be ordinary liquids, crystals, or glasses. How can we identify what state our system is in?

### 1.1.1 Mechanical differences

Shear strain in materials gives rise to stress, and we can identify materials based on the time-dependence of this stress. Stress in a solid does not decay in time, while stress in liquids relaxes (vanishes) over time. This is one way to say that liquids flow, and solids do not. The time dependence of stress - captured in the relaxation time - is particularly important in distinguishing between ordinary liquid, supercooled liquid, and glass.

### 1.1.2 Structural similarities

Crystals are uniquely known for their long-range translational order, which clearly distinguishes them from other materials. On the other hand, supercooled/ordinary liquids and glasses are not known to be structurally different from each other, so inspection is not sufficient to tell them apart.

### 1.1.3 Thermodynamic signatures

The liquid to crystal phase transition is a first order transition, so it leaves clear thermodynamic signatures in quantities such as the energy. The liquid to glass transition does not seem to be a phase transition, so it does not leave an obvious thermodynamic signature (Fig. 2). However, glass is so slow that non-vibrational degrees of freedom freeze out, leading to a calorimetric difference between liquids and glasses similar to that of liquids and crystals. We can see this when comparing the heat capacities of glass and liquid.

---

<sup>1</sup>I found Andrea Cavagna's review helpful in understanding the problem of supercooled liquids [3].

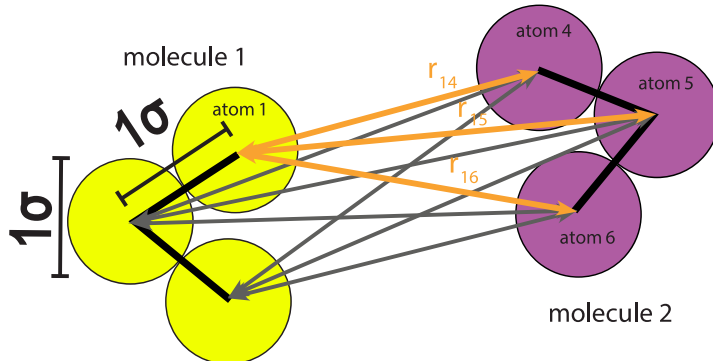


Figure 1: The model system consisted of molecules made from three soft disks which interacted with disks of other molecules. The vertex angle is held rigid at  $75^\circ$ .

## 2 Model details

The simulations consisted of systems of 2-D triatomic molecules (Fig. 1), analogous to the Lewis-Wahnström model for ortho-terphenyl [4]. We used a shifted, truncated, three-site Lennard-Jones pair potential. The cutoff distance was chosen to be  $r_c = 2.5\sigma$  by convention [1]. The potential had the explicit form given by Equation 1.

$$V(\mathbf{R}) = \sum_{\substack{j,k \\ j \neq k}}^N \sum_{a,b=1}^3 u(r_{ja,kb}), \quad r_{ja,kb} = |\mathbf{r}_{kb} - \mathbf{r}_{ja}| \quad (1a)$$

$$u(r) = \begin{cases} u_{LJ}(r) - u_{LJ}(r_c) & r \leq r_c \\ 0 & r > r_c \end{cases} \quad (1b)$$

$$u_{LJ}(r) = 4\epsilon[(\sigma/r)^{12} - (\sigma/r)^6] \quad (1c)$$

Simulations were carried out in the microcanonical (NVE) ensemble with square periodic boundary conditions, and the equations of motion were numerically integrated using the velocity Verlet algorithm [1]. Rotation was handled using RATTLE, a constraint dynamics algorithm that works with velocity-Verlet to satisfy bond-length constraints at every integration step [2]. Our time step was  $\delta t = 0.001\tau$ ,  $\tau = \sqrt{m\sigma^2/\epsilon}$ . Time-independent quantities are averaged over  $3 \times 10^5$  configurations. Time correlation functions are averaged over  $2 \times 10^5$  trajectories. Before taking any measurements, the system is "packed" and cooled to the density and temperature of interest, then given  $3000\tau$  to relax as long as reasonable. Thermodynamic parameters range among  $k_B T/\epsilon = \{0.2, 0.65\}$  and  $\rho\sigma^2 = 0.25$  ( $\phi = 0.589$ ).

## 2.1 Finite size

Thermodynamic phases are defined for infinite systems, so simulation accuracy benefits from an increasing number of molecules. A reasonable check for simulation accuracy is to compare results between simulations of differing size. If a change in system size does not change the results, then we can be more confident that the results are not artifacts of finite-size effects (Fig. 2).

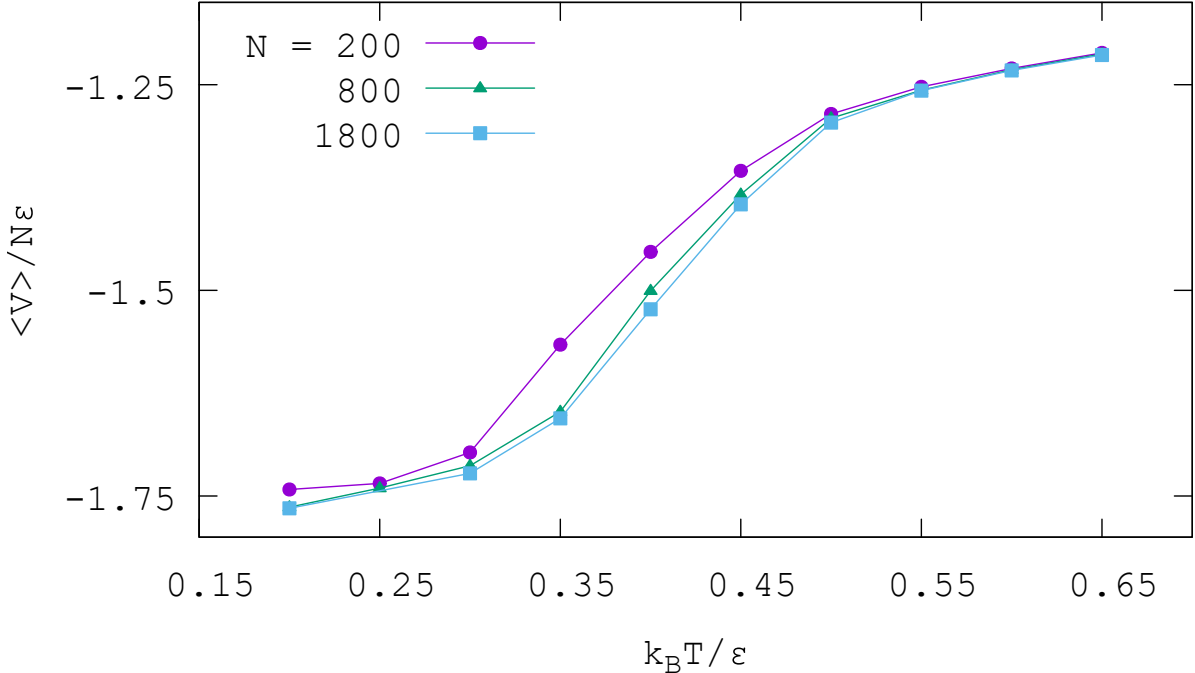


Figure 2: The figure plots potential energy per particle against temperature for different system size (number of molecules)  $N$ . This system is liquid at high temperature, glass at low temperature, and supercooled in-between. Averaged over  $3 \times 10^5$  configurations.

## 3 Structure

### 3.1 Looking at the configurations

I have isolated a few sample configurations of systems in different states (Fig. 3). Qualitative information like this was helpful in leading the direction of our inquiry.

### 3.2 Hexatic order

The hexatic order we refer to here is verbosely a six-fold body-orientational symmetry of molecules. In the hexatic body-orientationally ordered phase, molecules will line up along one of six favored directions (Fig. 3, 4): much like how the liquid crystalline nematic phase features two favored directions.

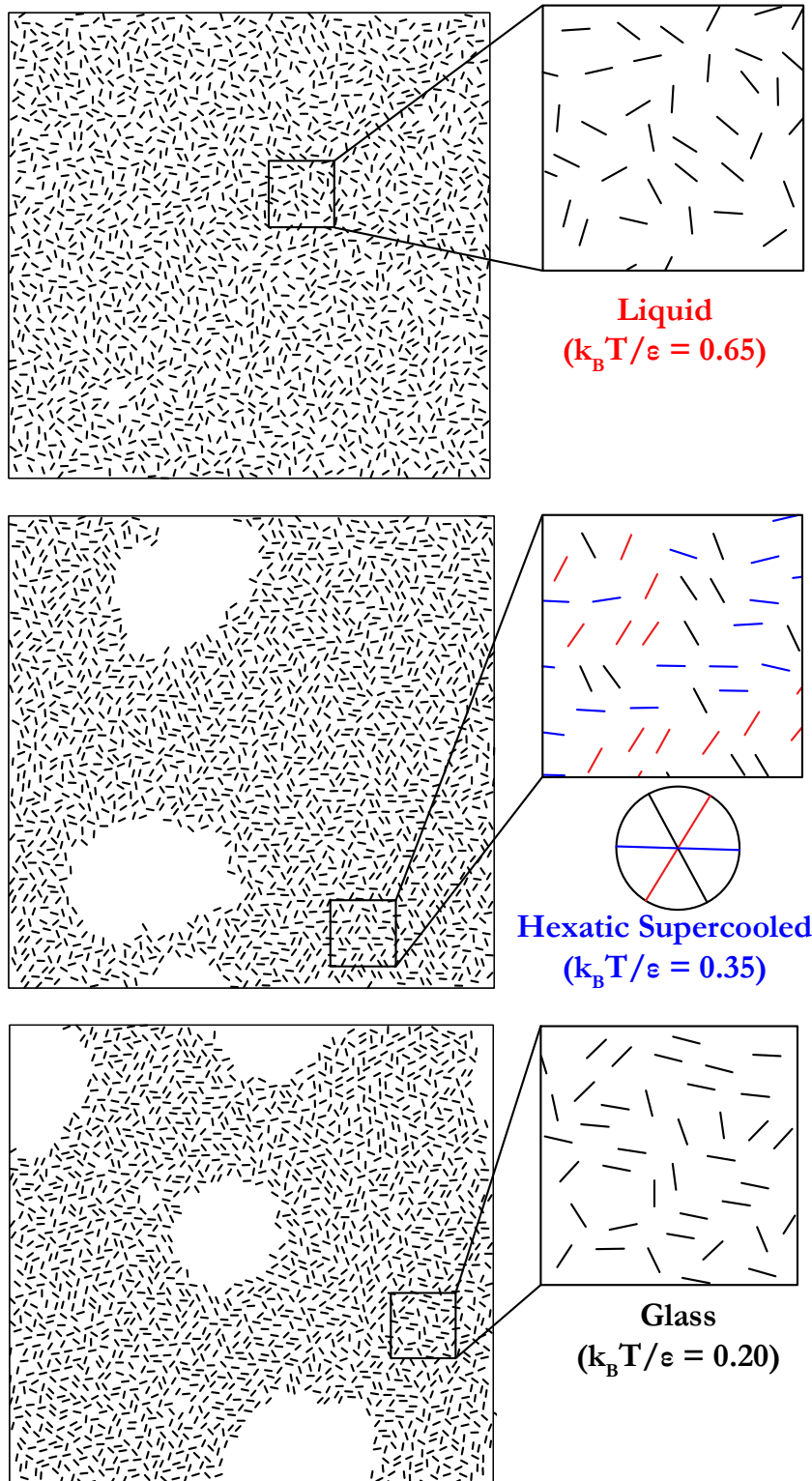


Figure 3: Sample configurations from our simulations at different temperatures,  $N=1800$ . Lines represent the orientation of molecules. The supercooled liquid appears to line up along six preferred directions.

The extent of hexatic order may be characterized by the hexatic order parameter  $s_6$ , given by:

$$s_6 = \frac{1}{N^2} \sum_{j,k=1}^N \cos(6\theta_{jk}) \quad (2)$$

The order parameter ranges from 0 to 1, disordered to ordered. Molecule  $k$  contributes most to  $s_6$  when it has an orientation parallel to molecule  $j$  or offset by an integer multiple of  $\frac{\pi}{3}$ . In this way,  $s_6$  picks out body-orientational symmetry in rotation by  $\frac{\pi}{3}$ .

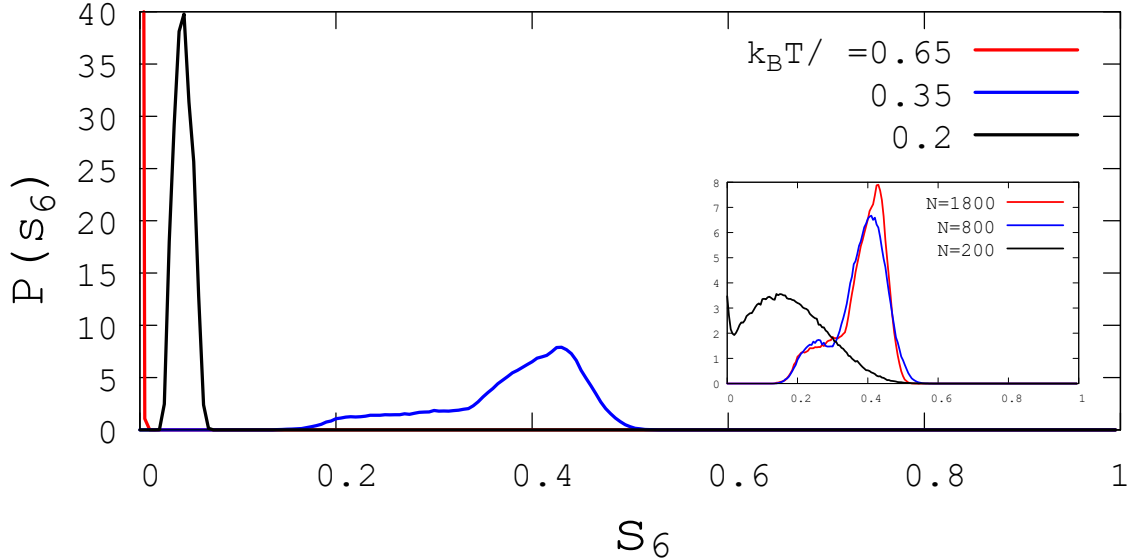


Figure 4: Probability distribution of the order parameter at different temperatures,  $N=1800$ . Averaged over  $3 \times 10^5$  configurations. Inset: The order parameter for different system size  $N$ . Note the persistence of order at different system sizes. Averaged over  $3 \times 10^5$  configurations.

### 3.3 Pair correlation functions

In studying the structure of a system, it is useful to understand how the molecules are distributed within the system. The radial distribution function  $g_2(r)$ , also called the pair correlation function, measures how local density changes with distance from a reference particle. The pair correlation function is formally an ensemble average (denoted by angle brackets) over pairs:

$$g_2(\mathbf{r}) = \frac{1}{N\rho} \left\langle \sum_j^N \sum_{k \neq j}^N \delta(\mathbf{r} - \mathbf{r}_{jk}) \right\rangle \quad (3)$$

$$= \frac{V}{N^2} \left\langle \sum_j^N \sum_{k \neq j}^N \delta(\mathbf{r} - \mathbf{r}_{jk}) \right\rangle \quad (4)$$

In practice, we calculate  $g_2(r)$  by assuming a homogeneous and isotropic liquid, so we can make the following simplification:

$$g_2(r) = \begin{cases} \frac{1}{N} \frac{1}{4\pi r^2 \rho} \left\langle \sum_j^N \sum_{k \neq j}^N \delta(r - r_{jk}) \right\rangle & \text{three dimensions} \\ \frac{1}{N} \frac{1}{2\pi r \rho} \left\langle \sum_j^N \sum_{k \neq j}^N \delta(r - r_{jk}) \right\rangle & \text{two dimensions} \end{cases} \quad (5)$$

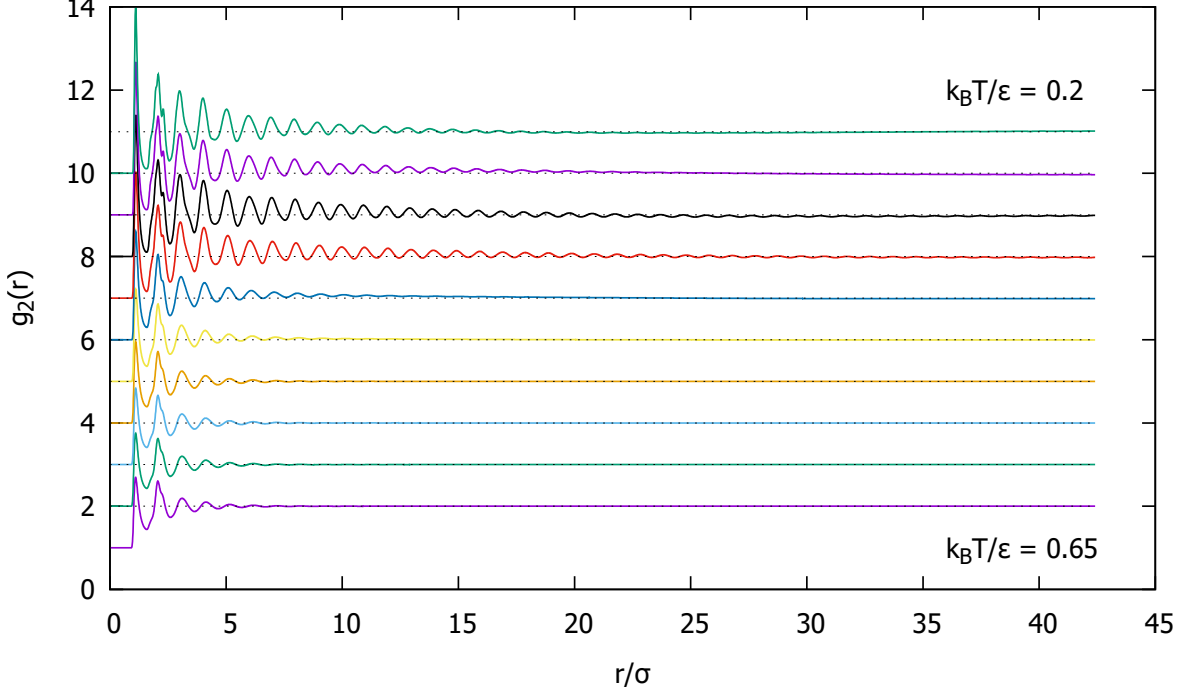


Figure 5: Site to site pair correlation function for the system of  $N=1800$  molecules. Averaged over  $3 \times 10^5$  configurations. Temperature increases by  $0.05 k_B T / \epsilon$  for each successive curve from the top. Curves are displaced vertically to improve visibility.

### 3.3.1 Hexatic pair correlation function

We also compute the hexatic pair correlation function, appending to the c.o.m-c.o.m pair correlation function a factor of  $\cos 6\theta_{jk}$ . The extra factor tells the correlation function to focus on molecules lined up with the favored directions, allowing us to determine a correlation length for the hexatic body-orientational order (Fig. 7). The hexatic pair correlation function is given by:

$$g_2(6\theta|r) = \frac{V}{N^2} \left\langle \sum_j^N \sum_{k \neq j}^N \delta(\mathbf{r} - \mathbf{r}_{jk}) \cos(6\theta_{jk}) \right\rangle \quad (6)$$

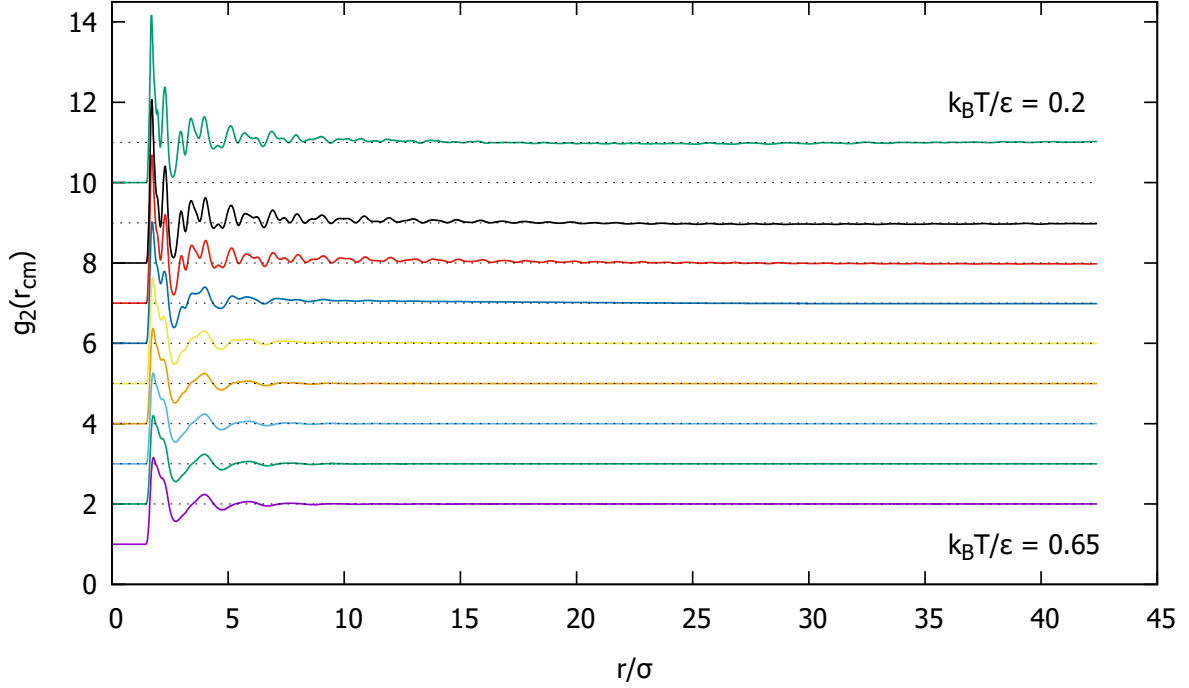


Figure 6: Center of mass to center of mass pair correlation function for the system of  $N=1800$  molecules. Averaged over  $3 \times 10^5$  configurations. Temperature increases by  $0.05k_B T/\epsilon$  for each successive curve from the top. Curves are displaced vertically to improve visibility. The 2nd curve from the top ( $k_B T/\epsilon = 0.25$ ) is missing due to corrupted data.

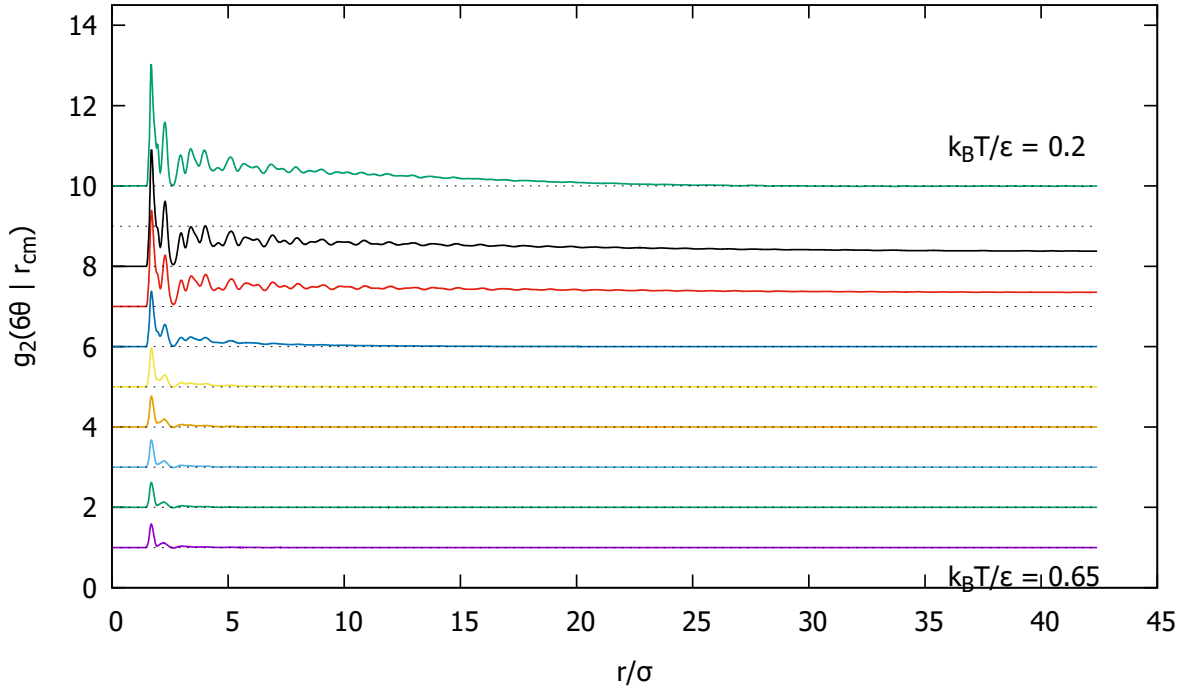


Figure 7: Hexatic body-orientational pair correlation function for the system of  $N=1800$  molecules. Averaged over  $3 \times 10^5$  configurations. Temperature increases by  $0.05k_B T/\epsilon$  for each successive curve from the top. Curves are displaced vertically to improve visibility. The 2nd curve from the top ( $k_B T/\epsilon = 0.25$ ) is missing due to corrupted data.



### 3.3.2 Static structure factor

The pair correlation function  $g_2(r)$  is closely related to the "static structure factor"  $\hat{S}(k)$  via a Fourier transform. As the Fourier transform of  $g_2(r)$ ,  $\hat{S}(k)$  can pick up on any periodicity in translational order - useful for finding lattice constants of a crystal, or short-range structure in a liquid. We compute the static structure factor (Fig. 8, 9) to rule out crystalline translational order and to find the ideal scattering momentum for other scattering functions like Equation 17.

The static structure factor is formally given by

$$\hat{S}(k) = \frac{1}{N} \left\langle \sum_{j,k=1}^N e^{-i\mathbf{k}\cdot(\mathbf{r}_j - \mathbf{r}_k)} \right\rangle \quad (7)$$

But in practice, we compute  $\hat{S}(k)$  in liquids by relating to  $g(r)$ :

$$\hat{S}(k) = 1 + \rho \int e^{-i\mathbf{k}\cdot\mathbf{r}} (g(r) - 1) d\mathbf{r} + N\delta_{\mathbf{k},0}$$

In two dimensions, it is given by

$$\begin{aligned} \hat{S}(k) &= 1 + \rho \int e^{-i\mathbf{k}\cdot\mathbf{r}} (g(r) - 1) d\mathbf{r} + N\delta_{\mathbf{k},0} \\ &= 1 + \rho \int e^{-ikr \cos \theta} (g(r) - 1) r dr d\theta \\ &= 1 + \rho \int \left[ \int e^{-ikr \cos \theta} d\theta \right] r (g(r) - 1) dr \\ &= 1 + 2\pi\rho \int_0^\infty J_0(kr) r (g(r) - 1) dr \end{aligned} \quad (8)$$

where we let  $\mathbf{k} \neq \mathbf{0}$  and  $J_0$  is a Bessel function:

$$J_n(x) = \frac{1}{2\pi} \int_{-\pi}^{\pi} e^{i(x \sin \tau - n\tau)} d\tau$$

For completion, in three dimensions it looks like:

$$\hat{S}(k) = 1 + 4\pi\rho \int_0^\infty r^2 \frac{\sin(kr)}{kr} (g(r) - 1) dr \quad (9)$$

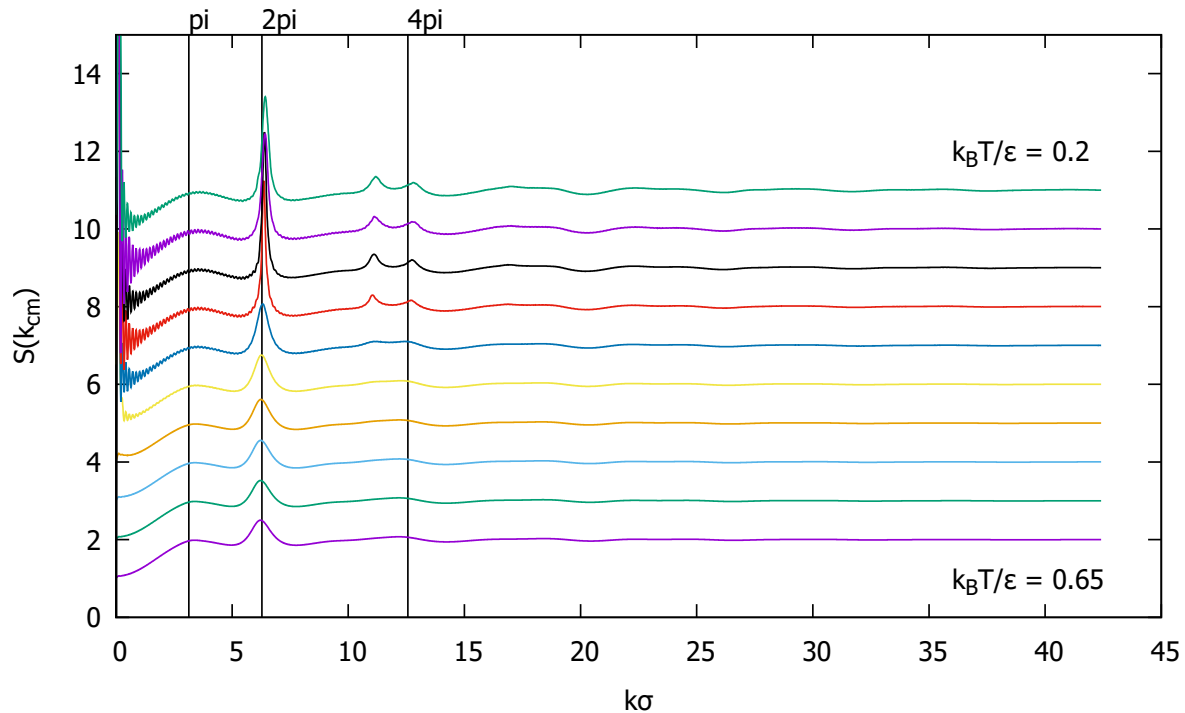


Figure 8: Site-site static structure factor via Fourier transform of the pair correlation function for the system of  $N=1800$  molecules. Averaged over  $3 \times 10^5$  configurations. Temperature increases by  $0.05k_B T/\epsilon$  for each successive curve from the top. Curves are displaced vertically to improve visibility.

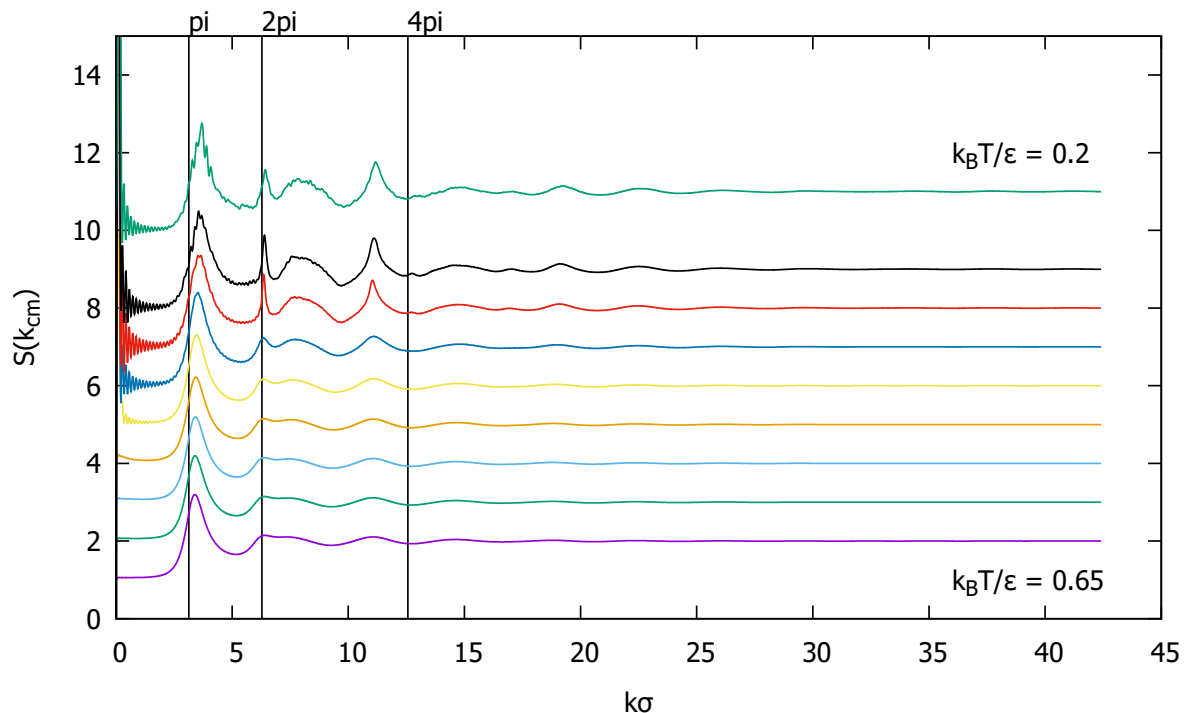


Figure 9: Center of mass static structure factor via Fourier transform of the pair correlation function for the system of  $N=1800$  molecules. Averaged over  $3 \times 10^5$  configurations. Temperature increases by  $0.05k_B T/\epsilon$  for each successive curve from the top. The 2nd curve from the top ( $k_B T/\epsilon = 0.25$ ) is missing due to corrupted data. Curves are displaced vertically to improve visibility.

## 4 Dynamics

### 4.1 Mean square displacement

The mean square displacement  $\langle \Delta r^2(t) \rangle$  is our go-to dynamical observable.  $\langle \Delta r^2(t) \rangle$  has clear physical significance, is easy to interpret, and is common in the literature. It is given by:

$$\langle \Delta r^2(t) \rangle = \frac{1}{N} \left\langle \sum_i^N (\mathbf{r}_i(\mathbf{t}' = \mathbf{t}) - \mathbf{r}_i(\mathbf{t}' = \mathbf{0}))^2 \right\rangle \quad (10)$$

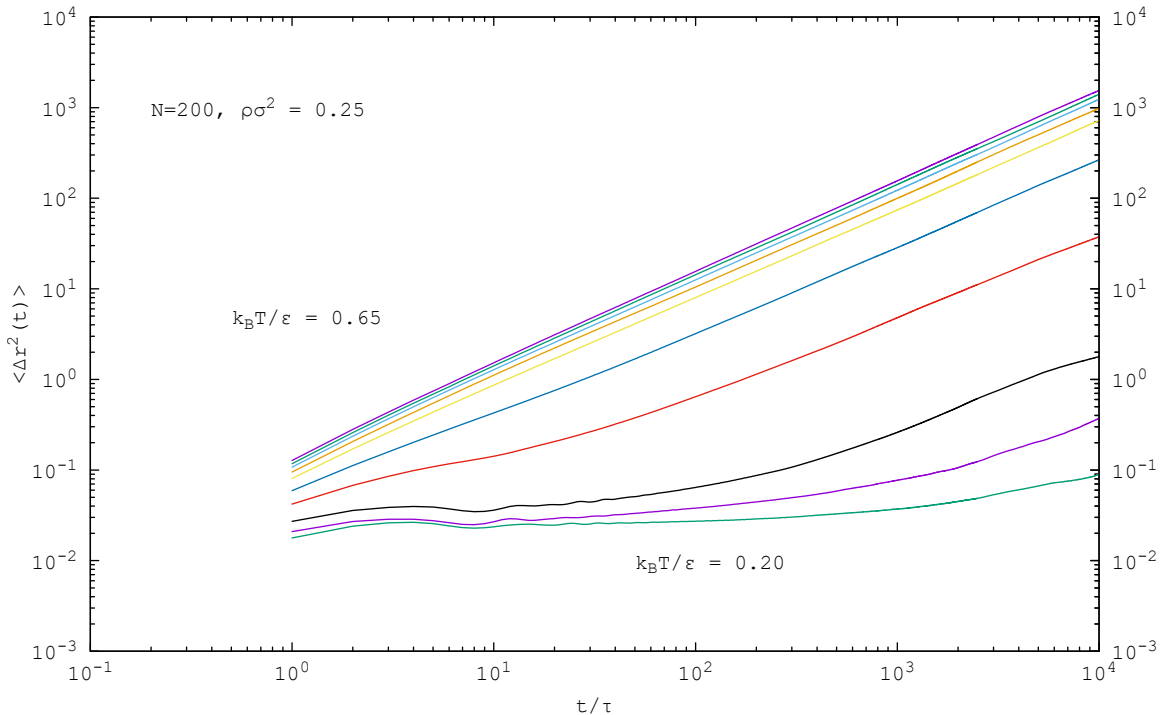


Figure 10: The mean square displacement of the  $N=200$  system at different temperatures. Averaged over  $2 \times 10^4$  trajectories.

#### 4.1.1 Calculating the diffusion coefficient

From the mean squared displacement we can extract the (self) diffusion coefficient  $D$ , a useful scalar summarizing the dynamics of the system. In particular, it is simply related to inverse viscosity so we can use it to track a liquid's progress through the supercooled and glassy regimes.

**Theorem 1.** *In  $d$  dimensions,  $\langle \Delta r^2(t) \rangle$  and  $D$  are related by the equation*

$$\frac{\partial \langle \Delta r^2(t) \rangle}{\partial t} = 2dD \quad (11)$$

One can derive this relation from the diffusion equation:

$$\frac{\partial \rho(\mathbf{r}, t)}{\partial t} = D \nabla^2 \rho \quad (12)$$

using Stoke's theorem:

$$\int_{\Omega_\infty} d\mathbf{r} (\mathbf{u} \nabla^2 \mathbf{v} - \mathbf{v} \nabla^2 \mathbf{u}) = \int_{\partial \Omega_\infty} d\mathbf{a} \cdot (\mathbf{u} \nabla \mathbf{v} - \mathbf{v} \nabla \mathbf{u}) \quad (13)$$

*Proof.* Let  $\mathbf{r}$  be a d-dimensional vector.

$$\begin{aligned} \langle (r(t) - r(t_o))^2 \rangle &= \int_{\Omega_\infty} d\mathbf{r} (\mathbf{r}(t) - \mathbf{r}(t_o))^2 \rho(\mathbf{r}, t) \\ \implies \frac{d}{dt} \langle (r(t) - r(t_o))^2 \rangle &= \int_{\Omega_\infty} d\mathbf{r} (\mathbf{r}(t) - \mathbf{r}(t_o))^2 D \nabla^2 \rho \\ &= D \int_{\Omega_\infty} d\mathbf{r} \nabla^2 ((\mathbf{r}(t) - \mathbf{r}(t_o))^2) \rho \\ &= 2dD \int_{\Omega_\infty} d\mathbf{r} \rho \\ &= 2dD \end{aligned}$$

□

Note that this relation is only true in the infinite time limit, so it is only valid at long times.

## 4.2 Body-orientational time correlation functions

To understand more about the dynamics of a system, we can do better than just the mean square displacement. There are many other correlation functions which give us quantitative information about the dynamical properties of the system.

The orientational correlation functions are constructed from the Legendre polynomials in three dimensions, and the Chebyshev polynomials in two dimensions. For our purposes, we use the Chebyshev polynomials:

$$T_n(\cos \theta) = \cos(n\theta)$$

The single molecule orientational time correlation function (orientational autocorrelation function) measures how much a tagged molecule's initial orientation is correlation with its orientation at some later time, given by:

$$C(t) = \left\langle \frac{1}{N} \sum_{j=1}^N T_2(\hat{\Omega}_j(0) \cdot \hat{\Omega}_j(t)) \right\rangle \quad (14)$$

$$= \left\langle \frac{1}{N} \sum_{j=1}^N [2(\hat{\Omega}_j(0) \cdot \hat{\Omega}_j(t))^2 - 1] \right\rangle \quad (15)$$

where  $\hat{\Omega}_j(t)$  is the unit orientation vector of molecule  $j$ .  $C(t)$  is written such that if the orientation of molecule  $j$  becomes uncorrelated with itself over time,  $\lim_{t \rightarrow \infty} C(t) = 0$ .

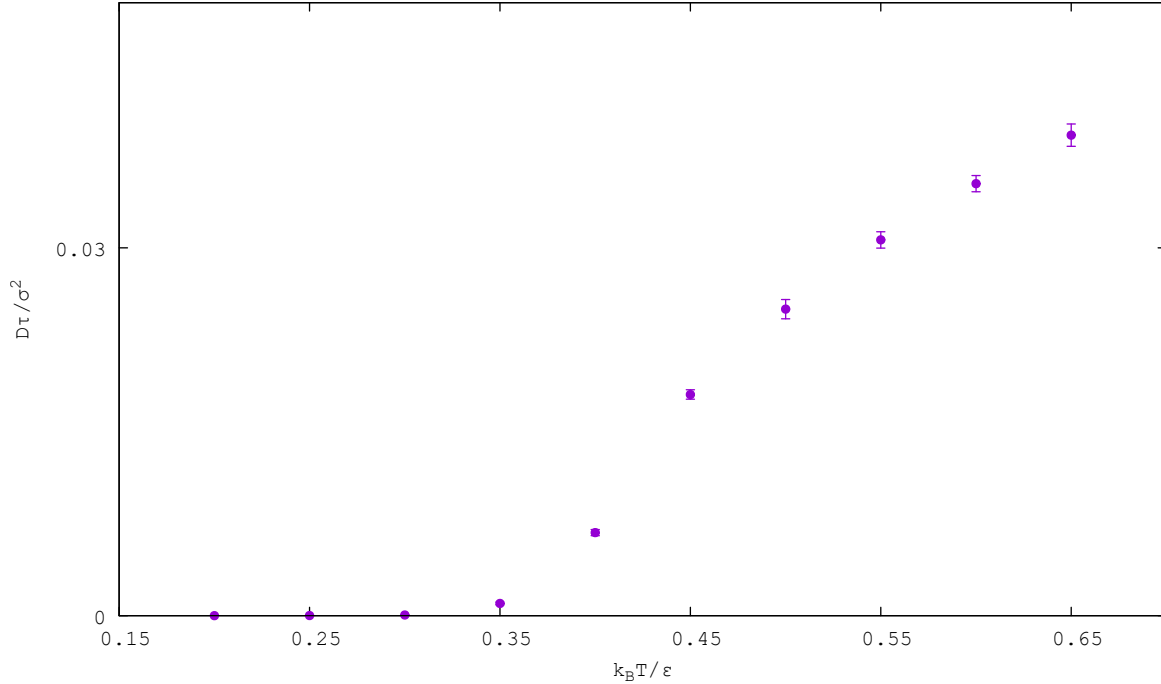


Figure 11: An "Angell plot" describes the viscosity (trivially related to the diffusion coefficient, plotted here) against temperature. The diffusion coefficient may be obtained by taking a time derivative of the mean square displacement (Figure 12). Averaged over  $2 \times 10^4$  trajectories.

#### 4.2.1 Single and collective hexatic body-orientational time correlation function

To study hexatic body-orientational relaxation times, we use the sixth Chebyshev polynomial to construct hexatic body-orientational time correlation functions. The single molecule hexatic body-orientational correlation function is given by:

$$C_s^6(t) = \left\langle \frac{1}{N} \sum_{j=1}^N T_6(\hat{\Omega}_j(0) \cdot \hat{\Omega}_j(t)) \right\rangle$$

while we define a collective analog by:

$$C_c^6(t) = \left\langle \frac{1}{N^2} \sum_{j,k=1}^N T_6(\hat{\Omega}_j(0) \cdot \hat{\Omega}_k(t)) \right\rangle \quad (16)$$

### 4.3 Incoherent intermediate scattering function

In the literature, another common dynamical observable closely related to the mean square displacement is the incoherent intermediate scattering function  $F_s(q, t)$ . Deeply supercooled liquids and glasses are known to exhibit what is called two-step relaxation in the mean square displacement and  $F_s(q, t)$ , so it is an invaluable tool in tracking the

glass transition in our simulations.

$$F_s(q, t) = \left\langle \frac{1}{N} \sum_{j=1}^N e^{i\mathbf{q} \cdot (\mathbf{r}_j(t) - \mathbf{r}_j(0))} \right\rangle \quad (17)$$

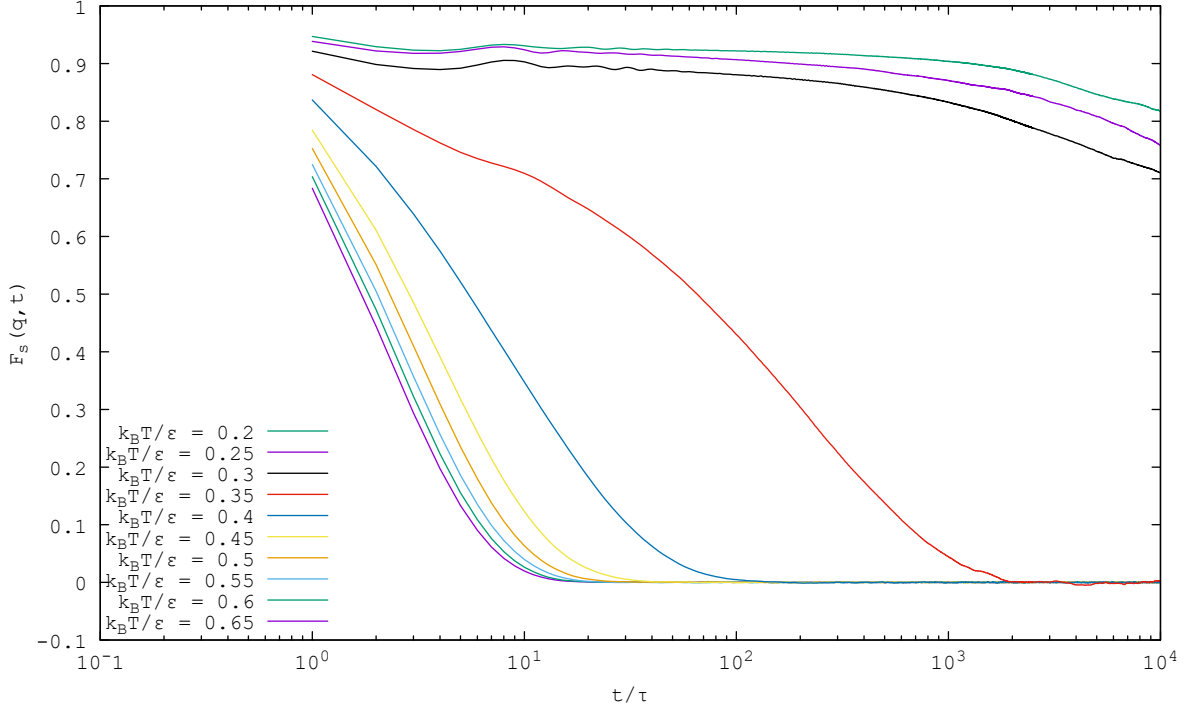


Figure 12: The figure plots the incoherent intermediate scattering function (ISF) as a function of temperature. ISF is a prevalent dynamical correlation function that can also "see" two-step relaxation in supercooled systems. Averaged over  $2 \times 10^4$  trajectories.

## References

- [1] M. P. Allen and D. J. Tildesley. *Computer simulation of liquids*. Oxford university press, 2017.
- [2] H. C. Andersen. Rattle: A velocity version of the shake algorithm for molecular dynamics calculations. *Journal of Computational Physics*, 52(1):24–34, 1983.
- [3] A. Cavagna. Supercooled liquids for pedestrians. *Physics Reports*, 476(4-6):51–124, 2009.
- [4] L. J. Lewis and G. Wahnström. Molecular-dynamics study of supercooled ortho-terphenyl. *Physical Review E*, 50(5):3865, 1994.